J. Physiol. (1976), **258**, *pp.* 547–577
With 14 *text-figures*
Printed in Great Britain

ANALYSIS OF PACE-MAKER AND REPOLARIZATION CURRENTS IN FROG ATRIAL MUSCLE

BY HILARY F. BROWN, ANNE CLARK AND SUSAN J. NOBLE

From the University Laboratory of Physiology, South Parks Road, Oxford OX1 3PT

(*Received 28 July 1975*)

SUMMARY

1. A quantitative analysis of the time-dependent component of outward membrane current in atrial wall trabeculae from *Rana catesbeiana* and *Rana ridibunda* has been carried out using a double sucrose gap technique.

2. Separation of the different components of delayed outward current was hampered by the sigmoid onset of one of the outward current systems $i_{x_{fast}}$ and by the development of potassium ion accumulation which prevented current activation from reaching a steady state at positive membrane potentials. Semilogarithmic analysis of positive current decay tails recorded immediately following square voltage clamp depolarizations was therefore used to separate the two membrane conductance components $i_{x_{fast}}$ and $i_{x_{slow}}$ and the third component, attributable to potassium ion accumulation, which was almost invariably present in the tails.

3. It is shown that inaccuracies in this method of semilogarithmic separation of components caused by visual assessment of the i_3 (accumulation) line are minor compared with the large changes in the time constants of $i_{x_{fast}}$ and more especially of $i_{x_{slow}}$ which would result from ignoring the potassium accumulation component.

4. Such semilogarithmic separation of the three components of outward current gave separate activation curves for each of the two membrane conductance components, $i_{x_{fast}}$ and $i_{x_{slow}}$.

5. Measurement of 'total' activation curves in which all components of outward current were represented could be made more easily and fairly reliably. The position and shape of these activation curves on the voltage axis were found to closely resemble those obtained by three component separation. It is therefore suggested that such a simplified analysis reflects the properties of the individual currents sufficiently well for it to be of use in preliminary studies of, for example, drug action.

6. The kinetic properties of the atrial outward currents have been

investigated over a wide potential range. Because of the presence of potassium ion accumulation, an indirect method of obtaining the average value of $1/\tau$ for outward current decay at negative potentials had to be employed.

7. It is shown that some degree of inward-going rectification is associated with the outward current systems of frog atrium.

8. The possible reasons for the differences between the analysis presented here and those presented earlier by us (Brown & Noble, 1969*a*, *b*) and by Ojeda & Rougier (1974) are discussed.

INTRODUCTION

In a previous paper (Brown, Clark & Noble, 1976*a*) we have presented evidence for the existence of two outward current systems in the membrane of preparations dissected from the atrial wall of *Rana catesbeiana* and *Rana ridibunda* ($i_{x_{fast}}$ and $i_{x_{slow}}$) whose time constants of decay at negative potentials are relatively short ($\tau_{x_{fast}}$ = *ca.* 300 ms, $\tau_{x_{slow}}$ = *ca.* 1·5 s at about −40 mV). The subscript x indicates that the currents concerned are probably not carried only by potassium ions. As we have shown, a third component of membrane current is also present. At comparable membrane potentials the time constant of decay of this component is very much slower than those of the outward conductance mechanisms (τ_3 varies between 5·0 and 18·0 s). We have outlined the reasons for supposing that this third current is not carried by time-dependent conductance channels but is due to potassium ions accumulating immediately outside atrial cell membranes, reasons which will be dealt with fully in the following paper (Noble, S. J., 1976).

The third current component ($i_{accumulation}$) develops noticeably during all but very short depolarizing voltage clamp pulses. In the current tails following sufficiently large and/or long depolarizations it is mixed with one or both of the other atrial outward currents. Separation of $i_{accumulation}$ from $i_{x_{fast}}$ and $i_{x_{slow}}$ can only be achieved by semilogarithmic analysis of positive current decay tails. Such an analysis, while it enables certain information about the characteristics of the individual activation curves $x_{fast}(E_m)$ and $x_{slow}(E_m)$ to be obtained, does not allow the kinetic behaviour of $i_{x_{fast}}$ and $i_{x_{slow}}$ to be quantified over a wide range of membrane potentials. Moreover, it will be shown that the presence of potassium accumulation introduces additional factors which make it impossible to define accurately all the voltage-dependent behaviour of the atrial plateau conductances. In the case of the activation curves, $x_{fast}(E_m)$ and $x_{slow}(E_m)$, the shape of the relationships at positive membrane potentials is uncertain and separation of the two fully activated current–voltage relations,

$\bar{i}_{x_{fast}}(E_m)$ and $\bar{i}_{x_{slow}}(E_m)$, cannot be attempted. (The symbol $\bar{i}$ is that now generally used to indicate fully activated current, i.e. the current which crosses the membrane when all the conductance channels are open, see Noble, 1972). Thus there are obstacles which prevent a complete Hodgkin–Huxley analysis of these components of delayed rectification in atrium.

Nevertheless the close resemblance apparently existing between induced atrial and natural sinus pace-maker mechanisms (see Discussion; also Brown *et al.* 1976*a*) has encouraged us to press the analysis of this system as far as is practically possible. We shall attempt to show that quantitative information can be obtained that may be used to produce a simplified account of the outward conductance mechanisms, an account which is relevant in assessing their physiological role. This approach has already proved valuable when investigating the mode of action of adrenaline on the atrial pace-maker system (Brown & Noble, 1974) and it is hoped that its use may be extended in the future to the study of other drugs which affect cardiac rhythmicity.

METHODS

Atrial trabeculae having a diameter of approximately 150 μm were dissected from the endocardial surface of *R. catesbeiana* and *R. ridibunda* and investigated using a double sucrose gap technique. Full details of the method used are given in a previous paper (Brown *et al.* 1976*a*).

RESULTS

Information from current onsets

Once the atrial pace-maker current, i_p, had been identified with a component of delayed rectification $i_{x_{slow}}$ (see Brown *et al.* 1976*a*) we turned to the determination of the range of potentials over which this current is activated and of its rate of activation at different potentials. Our first approach was to observe the rate and amplitude of current onset during a voltage clamp depolarization. As described previously, analysis of the current decay tails after a clamp pulse reveals two components of delayed rectification ($i_{x_{fast}}$ and $i_{x_{slow}}$) together with a component of potassium ion accumulation ($i_{accumulation}$). Analysis of current characteristics from current onsets in multi-component systems can be made if two conditions are fulfilled: firstly, current activation must reach a steady state during the voltage clamp pulse, and secondly, if more than one current component is activated, the various onsets must be of known form (most simply exponential).

On examining the current onsets during voltage clamp pulses, we found, however, that if the depolarization took the membrane to potentials more

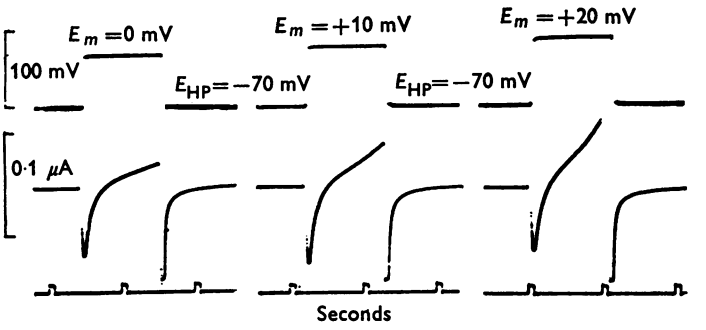

Fig. 1. Voltage clamp depolarizations of approximately 1·0 s duration given from a holding potential of −70 mV. Upper trace: the voltage record. Reading from left to right pulse magnitudes are +70, +80 and +90 mV. Lower trace: the corresponding current records. In all cases there is an initial inward current (downward deflexion) which, since the experiment was performed in Ringer + tetrodotoxin (TTX, 2×10^{-6} g/ml), must represent the onset and decay of the second inward Ca^{2+}/Na^{+} current. Following inactivation of this current outward current activation is recorded (upward deflexion). Its activation pattern appears to be virtually exponential during the +70 mV pulse but becomes definitely sigmoid during the +80 and +90 mV pulses.

Fig. 2. *A*, voltage clamp records obtained in Ringer + TTX (2×10^{-6} g/ml). Upper trace: current onset in response to a voltage clamp depolarization given from $E_{HP} = -40$ mV to $E_m = 0$ mV for 7·0 s. An upward deflexion represents outward current. Middle trace: positive (outward) current decay tails recorded after repolarization from $E_m = 0$ mV to the holding potential of −40 mV. Depolarization times to E_m were 500 ms, 1·0 s, 1·5 s, 2·0 s, 3·0 s, 4·0 s, 5·0 s and 7·0 s and these records were superimposed by tracing from the original pen recordings. Also shown is the onset corresponding to the 1·0 s depolarization as it was recorded at this higher amplification and the vertical interrupted lines indicate the repolarization points for the 500 ms and 1·0 s clamp pulses. It will be noted that net outward current (upward deflexion) is not recorded following such relatively short depolarizations for some time (see text). The horizontal interrupted line gives the steady-state current level at −40 mV. Note that, following the 7·0 s depolarization, the repolarization tail is much smaller and is beginning to reverse sign. Lower trace: the corresponding voltage record.

B, the current decay tails shown in Fig. 2*A* (middle trace) together with a number of others obtained in the same experiment have been separated semilogarithmically into two components $i_{x_{fast}}$ and ($i_{x_{slow}} + i_{accumulation}$). The absolute magnitude of these currents after depolarization time t is plotted here: crosses represent $i_{x_{fast}}$, filled circles ($i_{x_{slow}} + i_{accumulation}$). The shape of these 'envelopes of tails' should reflect the activation pattern of the plateau currents. Thus $i_{x_{fast}}$ appears to be a sigmoid function of E_m while $i_{x_{slow}}$ is an exponential one.

N.B. The *decrease* in the magnitude of the currents activated at long times is expected (see text).

positive than between −10 and zero mV, the current activated did not reach a steady state, but continued to increase for as long as the pulse was applied (Fig. 2*A*). This effect can be explained by the potassium accumulation hypothesis as will be shown in another paper (Noble, 1976).

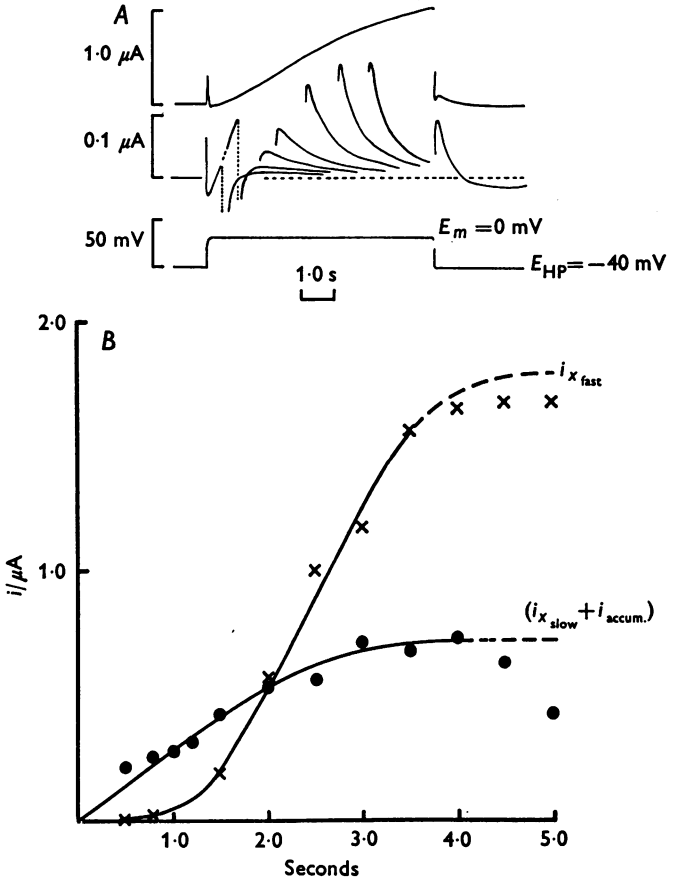

Fig. 2. For legend see facing page.

Further examination of the current onsets showed that not all of these were of simple form. Thus in Fig. 1 are shown responses to three depolarizing pulses. In each of these the current during the pulses shows an initial phase consisting of the development and subsequent inactivation of an inward current. This relatively slow, TTX-insensitive current is the Ca^{2+}/Na^+ or second inward current (Rougier, Vassort, Gargouil & Corabeuf, 1969). In addition the records show subsequent activation of outward current. It would appear that in response to the +70 mV pulse

(E_m = 0 mV), this onset is virtually exponential. However, in response to the +80 mV (E_m = +10 mV) and +90 mV (E_m = +20 mV) depolarizations, outward current onset is definitely sigmoid. This sigmoid pattern probably has nothing to do with the inactivation of the inward current which is completed within 250 ms, that is, before activation of the outward current becomes significantly non-exponential. Despite the fact that a residual amount of second inward current remains activated at all potentials (Besseau, 1972) it nevertheless appears that at least one of the outward currents must have a sigmoid onset.

Current decay tails are shown in Fig. 2*A* recorded after depolarizations of constant magnitude but increasing duration. These tails were separated semilogarithmically into two components, one consisting of $i_{x_{slow}}$ together with $i_{accumulation}$ and the other composed of $i_{x_{fast}}$. The peak amplitudes of these currents were then plotted against the duration of the preceding pulse (envelope of tails). The delay in appearance of $i_{x_{fast}}$ in the current tails following pulses of increasing duration reflects the time taken for it to be activated at the positive potential (E_m = 0 mV). Thus, the onset of $i_{x_{fast}}$ is given by the shape of its current tail envelope which is definitely sigmoid, whereas the onset of $i_{x_{slow}}$ is apparently exponential (Fig. 2*B*). The error introduced by separating the current tails into two rather than into three components affects mainly the time constant and therefore the magnitude of $i_{x_{slow}}$ (see Brown *et al.* 1976). Some effect on these parameters for $i_{x_{fast}}$ will also occur but this cannot account for the delay in onset shown here. Caution must, however, be used when interpreting this result since the large negative current immediately following short depolarization pulses (Fig. 2*A*; note the position of the vertical interrupted lines) could obliterate the presence of $i_{x_{fast}}$ in such tails. Further evidence that the onset of $i_{x_{fast}}$ is sigmoid is therefore presented below (see Discussion).

As Hodgkin & Huxley (1952) have demonstrated the equation for describing a time-dependent conductance is

$$\Delta i_x = \bar{i}_x . \Delta(x^\gamma), \tag{1}$$

where γ is a power which will be greater than 1 if more than one membrane reaction is required to open a conductance channel to the passage of ions. The finding that not all the current onsets are separable by semilogarithmic analysis into exponential form indicates that $\gamma > 1$ for at least one of the processes we are considering.

Thus, there are two obstacles to simple analysis of current onsets. Firstly, the onsets do not reach a steady state and secondly, the underlying membrane processes are such that the onsets cannot be simply separated. For these reasons we turned to the analysis of current decay.

Information from current decay

Fortunately, whatever the value of γ, the deactivation of a time-dependent conductance described by Hodgkin–Huxley kinetics is always exponential (Hodgkin & Huxley, 1952). Therefore we have analysed current decay tails. Fig. 3 shows a composite activation curve for all outward current systems which was obtained by measuring the total height

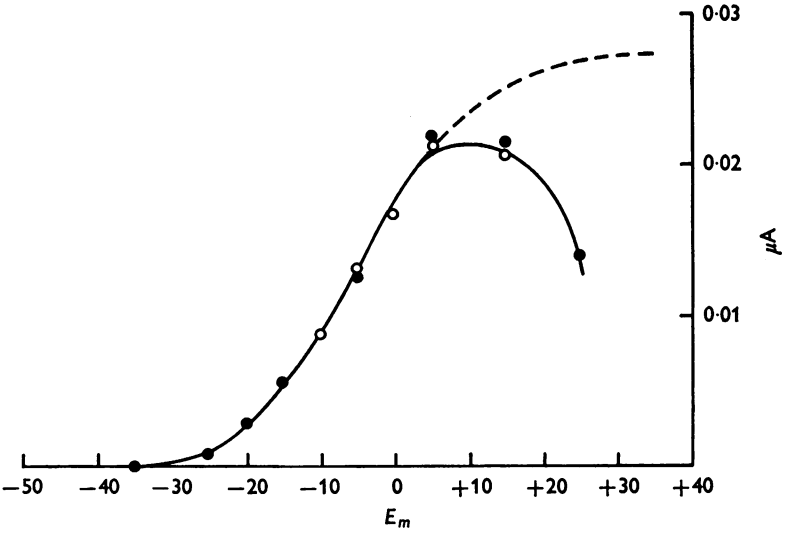

Fig. 3. Composite activation curve for the i_x systems obtained from an envelope of tails analysis, where $E_{HP} = -35$ mV and all pulses to E_m were applied for 10·0 s. The filled symbols are values obtained as the magnitude of the depolarizing pulse was increased, the open symbols as it was subsequently decreased. The interrupted line is included to show the shape that such a curve would normally be expected to have. For further discussion see text.

of the positive tail following depolarizing pulses of 10 s duration given from a holding potential of -35 mV. When the magnitude of the depolarizing pulse was increased beyond $+40$ mV, the heights of these tails progressively diminished. Subsequent activation curves obtained in a way which will be described below, led us to conclude that the real curve for i_x activation should have continued in the direction indicated by the interrupted line. The fact that it did not do so suggests that accumulation becomes large at membrane potentials positive to $+5$ mV. But, as will be shown, allowance can be made for this and a fuller quantitative analysis of current decay tails can be attempted.

For reasons which will become apparent, we have found it necessary to

investigate the behaviour of the outward time-dependent conductances above and below the reversal potential of $i_{x_{slow}}$ by different methods. We will refer to these methods as positive and negative tail analysis and will begin by considering the former.

1. *Positive tail analysis*

The envelope enclosing the maximal current activated during clamp pulses of a given amplitude but increasing duration should give the time course of activation at the potential to which the membrane was clamped (cf. Noble & Tsien, 1968). Although this method of 'envelope of tails' analysis was satisfactory for estimations of the atrial i_x systems for pulses of small amplitude (E_m lying comparatively close to E_R), when depolarizing pulses to potentials more positive than about -10 mV were used, the pulse tail amplitude did not reach a steady level but, as the pulse duration was prolonged, declined rapidly (Fig. 2*A*) and finally reversed sign becoming negative (see Noble, 1976, Fig. 5). It was therefore not possible to measure directly the maximum current activated at those potentials and estimations had to be made.

The use of the 'double pulse technique' in which $E_{HP} = E_R$ and the membrane is first depolarized to E_{m_1} and then repolarized to $E_{m_2}(< E_{HP})$ (see Brown *et al.* 1976*a*, Fig. 7) was limited for 'envelope' analysis because the slow development of accumulation current following repolarization to a potential positive to about -50 mV tended, in many experiments, to mask partially the decay of the i_x currents. The more conventional method of applying single voltage clamp pulses which started from and returned to the same holding potential had the advantage that a steady-state level of accumulation at E_{HP} could be allowed to develop before test pulses were applied. Such single voltage clamp pulses repolarizing to between about -50 and -20 mV produced positive current tails. In some preparations, if the depolarizing pulse was not applied for too long, the positive current decayed as a single or double exponential (Brown *et al.* 1976*a*, Figs. 8, 9*A* and *B*). However, even after short (500 ms) depolarizing pulses, other preparations gave positive tails which did not decay in the way which would be predicted if the only deactivating currents were $i_{x_{fast}}$ and/or $i_{x_{slow}}$. When large depolarizing pulses, longer than about 1·0 s, were applied to any preparation, the decay tail began to contain the third component of outward current.

A. Analysis of total current tails. Total current tail analysis may be performed quickly and easily and measures the total amount of outward current activated at a given value of E_m. As has already been implied (Brown *et al.* 1976*a*) the time-dependent potassium conductance normally activated by individual action potentials will be chiefly $i_{x_{slow}}$, although

very small amounts of $i_{\text{accumulation}}$ and $i_{x_{\text{fast}}}$ may also be present. In a given preparation the properties of $i_{x_{\text{slow}}}$ must be an important parameter in controlling repolarization and pace-maker activity. It therefore seemed important to determine how closely a 'total' current analysis, which unavoidably incorporates the properties of $i_{x_{\text{fast}}}$ and $i_{\text{accumulation}}$, may be used as a guide to the behaviour of $i_{x_{\text{slow}}}$ alone.

The experimental method for obtaining the total current activation curve, $x_{\text{total}}(E_m)$, was as follows. On a holding potential negative to the activation range for either plateau current, square voltage clamp depolarizations of varying magnitudes were superimposed. For a given depolarization value, E_m, the duration of the pulse was gradually increased until the current tails either reached a steady-state magnitude (following small depolarizations) or began to decline (after large depolarizations). Curves of $i_{x_{\text{total}}}$ against time were plotted (current tail 'envelopes') for the different values of E_m. A series of such plots from a typical experiment is shown in Fig. 4. The holding potential in this experiment was -55 mV and it can be seen that the 'envelopes' for $i_{x_{\text{total}}}$ resulting from depolarizations to $E_m = -45$, -35 and -25 mV (Fig. 4*A*) have approximately exponential patterns and reach a steady-state amplitude after pulse durations of between 5·0 and 10·0 s. This implies that only $i_{x_{\text{slow}}}$ together with comparatively small amounts of $i_{\text{accumulation}}$ are activated at these relatively negative potentials (see Fig. 2*B*). Larger depolarizations (E_m between -15 and $+35$ mV in 10 mV steps) give rise to sigmoid 'envelopes' which reach a peak and then decline so that it is necessary to extrapolate to the steady-state condition (interrupted lines in Fig. 4*B* and *C*). Clearly such extrapolations can introduce error and to minimize this it is sometimes necessary to take two possible values for steady-state activation and average them (see 'envelope' of tails for $E_m = +35$ mV). If we assume that the total amount of activation (Δx) by any given pulse is equal to the amount of subsequent deactivation, the peak values for such a series of curves (actual or extrapolated) gives $x_{\text{total}}(E_m)$ for all the outward current activated over the selected potential range. The $x_{\text{total}}(E_m)$ relation for the experiment illustrated in Fig. 4 is shown in Fig. 5*A*. Fig. 5*B* shows three activation curves obtained in the same way in three other preparations and it can be seen that though the threshold of activation of the i_x systems varies somewhat, the general shape of these curves in relation to their position on the voltage axis is, considering the inevitable errors involved, reasonably similar.

It will be noted that in Fig. 4 each current tail 'envelope' is labelled with a τ value. This value was obtained by determining the time taken for the i_x system to reach $(1-1/e)$ of its final magnitude at the depolarized potential, E_m. Inaccuracies will be involved where E_m is very positive, not

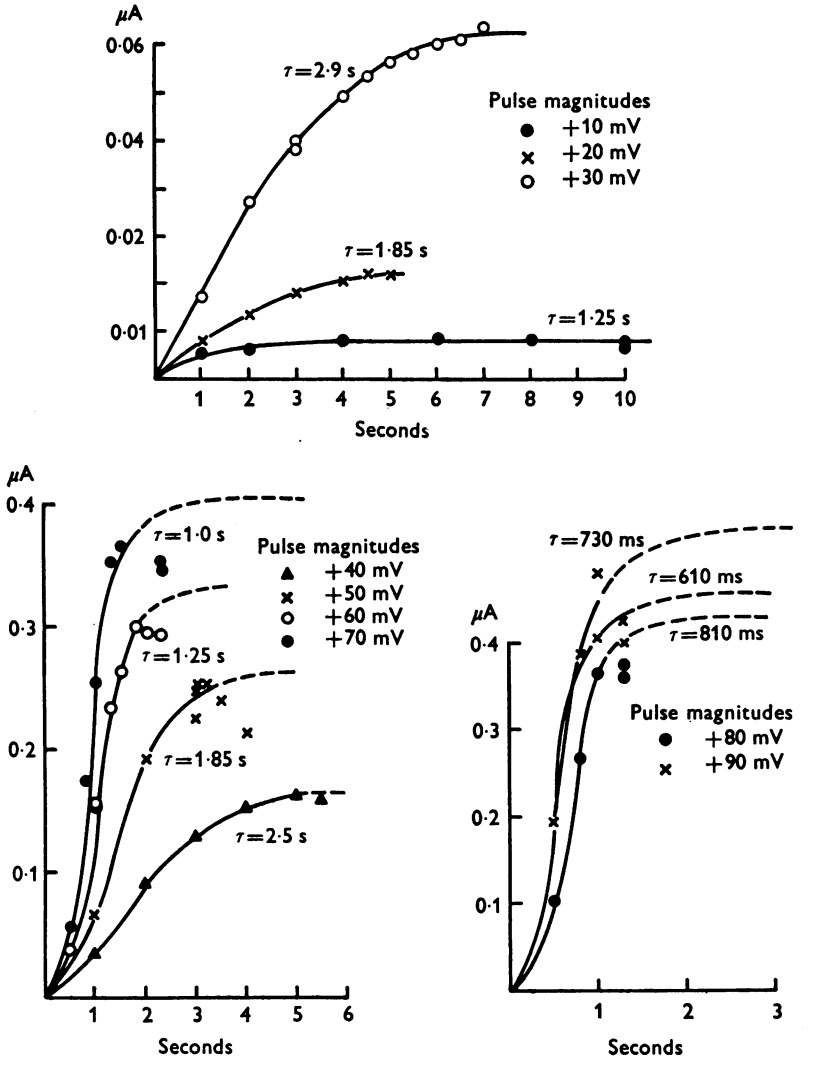

Fig. 4. Envelope of tails analysis designed to give x_{total} (E_m) carried out from a holding potential of -55 mV for values of E_m varying between -45 and $+35$ mV inclusive. *A*, depolarizations to -45, -35 and -25 mV. Note that current onset appears to be exponential and that the 'envelopes' reach a steady-state value indicating that current activation is complete for these values of E_m. *B*, depolarizations to -15, -5, $+5$, and $+15$ mV. Note that the current activation now appears to be a sigmoid function of E_m and that in all cases steady-state activation has had to be obtained by extrapolation (interrupted lines). *C*, depolarizations to $+25$ and $+35$ mV. Potassium ion accumulation now causes the tail height to fall so rapidly ($t \leqslant 1{\cdot}0$ s) that the accuracy of any extrapolation becomes very doubtful. For this reason two values have been estimated for $E_m = +35$ mV and their average value taken to represent full activation at this potential. Nevertheless we must regard the top of activation curves obtained by this method as approximate only.

only because extrapolation of the tail 'envelope' is needed, but also because its rise pattern is sigmoid. However, the values of τ_x so obtained give an approximate quantitative estimate of the kinetic behaviour of the total outward current activated in the plateau range of membrane potentials. Additional examples are plotted in Figs. 8 and 13.

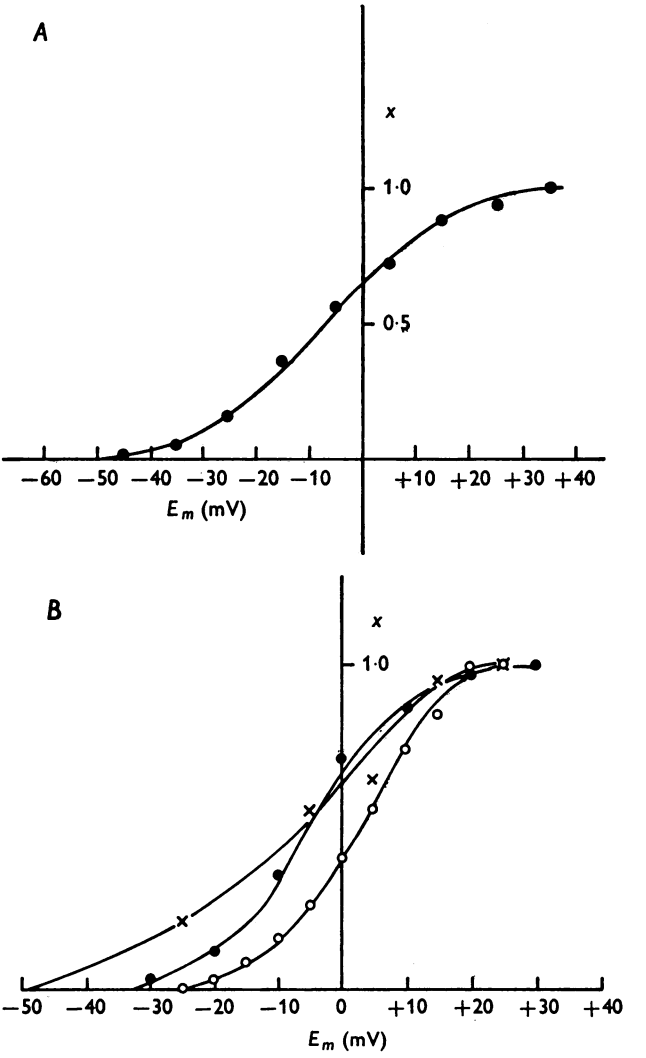

Fig. 5. Normalized estimates of $x_{total}(E_m)$ obtained by envelope of tails analysis. *A*, single activation curve obtained for the preparation which gave the results shown in Fig. 4. *B*, three other activation curves obtained in different preparations. Note that although x appears to approximate to 1 between about +20 and +35 mV, this value depends on the validity of the extrapolations in Fig. 4.

B. Three component analysis of current tails. The second type of analysis of positive current tails which might be expected to give a much more comprehensive account of the behaviour of the components involved, is time-consuming to perform by hand. The experimental method involved

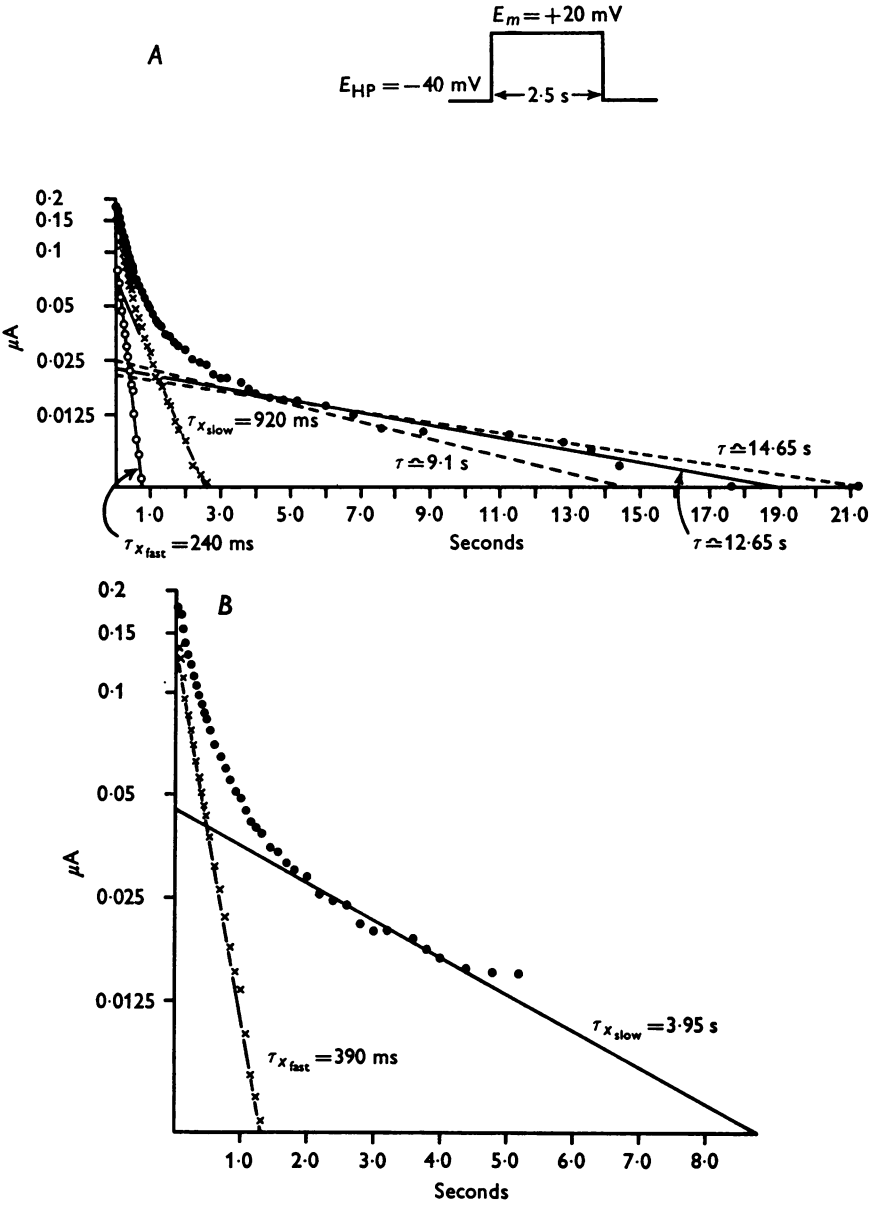

Fig. 6. For legend see facing page.

is identical to that just described, but here each current decay tail is fully separated semilogarithmically into three components. The principle of this analysis has already been described in the preceding paper (Brown *et al.* 1976*a*). Here we shall show how this analysis can be used to obtain activation curves. The tails following the longer duration pulses are used where necessary to obtain the approximate time constant of decay of the accumulation current. Fig. 6*A* shows how exponential subtraction of this very slowly decaying third component from the semilogarithmic plot of such a positive tail leaves two other components, $i_{x_{fast}}$ and $i_{x_{slow}}$. In this case the holding potential was -40 mV and a depolarizing pulse of $+65$ mV was superimposed upon it for 2·5 s. When a small amount of an accumulation current, decaying here with a time constant of approximately 12·65 s, is first subtracted from the tail, the time constants of the remaining conductance components becomes $\tau_{x_{fast}} = 240$ ms and $\tau_{x_{slow}} = 920$ ms. The value for $\tau_{x_{slow}}$ agrees well with the time constant of decay of the pacing current which, when clamped directly after an action potential, was 900 ms at the same holding potential (i.e. at -40 mV).

It will be seen from Fig. 6*A* that nearly all the points which represent the decay of the accumulation component alone are no greater than 0·015 μA positive to the base line and it may be wondered whether such small deviations can be measured sufficiently accurately especially when, as was done here, the line of best fit is drawn by eye. Complete accuracy is, of course, impossible but two important features are demonstrated in Fig. 6.

Firstly, two interrupted lines have been drawn in Fig. 6*A* which represent the extremes within which the line of best fit for the accumulation component must certainly be. These extremes correspond to time constants of decay of i_3 of 14·65 s and 9·1 s and the associated values for $\tau_{x_{slow}}$ which would be obtained on subtraction of these 'extreme' i_3 values

Fig. 6. Semilogarithmic analysis of positive current decay tails designed to obtain independent estimates of $x_{slow}(E_m)$ and $x_{fast}(E_m)$. *A*, the total current decay tail (filled symbols) is separated into three exponentially decaying components. A very slow component $i_{accumulation}$ ($\tau = 12{\cdot}65$ s) and two relatively rapidly deactivating components ($\tau_{x_{slow}} = 920$ ms (crosses) $\tau_{x_{fast}} = 240$ ms (open circles)). Note that the time constant of decay of $i_{x_{slow}}$ obtained in this way is very close to that of the directly clamped pace-maker current recorded at the same holding potential ($E_{HP} = -40$ mV). The interrupted lines and associated time constants give the apparent limits for the decay of the accumulation component (see text). *B*, the same current tail shown in Fig. 6*A* separated bi-exponentially. In order to do this the latter points in the decay tail have been ignored as these represent deviations from the base line of no more than 0·015 μA. $\tau_{x_{slow}}$ is now 3·95 s and $\tau_{x_{fast}}$ is 390 ms.

are 1·06 s and 900 ms, both values lying within 15% of the $\tau_{x_{slow}}$ (920 ms) obtained by subtraction of the i_3 line of best fit (the values of $\tau_{x_{fast}}$ remain unaltered).

The second important feature is well illustrated in Fig. 6*B*. Here, it is shown that if the last 0·015 μA of current decay is ignored and the same current tail is separated into only two exponential processes, $\tau_{x_{fast}}$ is increased by 64% to 390 ms while $\tau_{x_{slow}}$ is increased by 329% to 3·95 s. This huge difference in $\tau_{x_{slow}}$ illustrates the price of ignoring the accumulation current.

When the decay tails have been separated into three components, activation curves for the two conductance systems, $x_{fast}(E_m)$ and $x_{slow}(E_m)$ can be plotted by using the 'envelope of tails' method described above. Fig. 7*A* shows the activation curves obtained for one experiment analysed in this way. The interrupted line represents $x_{slow}(E_m)$ and the dotted line $x_{fast}(E_m)$. These are non-normalized activation curves and it can be seen that though the threshold of activation of $i_{x_{slow}}$ is more negative than that of $i_{x_{fast}}$ (a general finding in our experiments), the relative magnitude of the curves shows that at full activation the ratio $i_{x_{fast}}:i_{x_{slow}}$ is about 1·4:1. Also shown here is the activation curve for the total current, $x_{total}(E_m)$, (continuous line), and the maximum quantity of accumulation current (dot-dash line) subtracted at each value of E_m, which, for want of better terminology, may be referred to as $i_{accumulation}$ (E_m). It should not, however, be confused with an activation curve.

In Fig. 7*B* the activation curves resulting from these two methods of analysis ('total' and 'three component') are shown together. The curves for $x_{total}(E_m)$, $x_{slow}(E_m)$ and $x_{fast}(E_m)$ have all been normalized (i.e. x, the degree of activation, has been adjusted so that it varies between 0 and 1) and are shown on the same graph. It is very encouraging that the position occupied by the three normalized curves on the voltage axis should be so similar. This means that a change in position or shape of, for example, $x_{slow}(E_m)$ would almost certainly be reflected in a similar change in $x_{total}(E_m)$, so that studying the latter which is relatively easily done, may give indication of changes in the former.

Because of the prolonged nature of the analysis, tails from only two experiments have been separated into three components but in these E_m covered the majority of the i_x activation range. Data from other experiments, in which only a few values of E_m were investigated, support these conclusions.

C. Kinetic information from positive tails. In relation to Fig. 4 it was explained how the approximate time constant of activation of $i_{x_{total}}$ at positive membrane potentials could be obtained from the 'envelopes' of current tails following depolarizing pulses. Therefore, when $i_{x_{slow}}$ is

separated by three component analysis, this method may be used to obtain its activation time constant at given values of E_m. If the i_x current systems obey Hodgkin–Huxley kinetics then the rate constants $1/\tau$ at different potentials should show a typical U-shaped relation (Hodgkin &

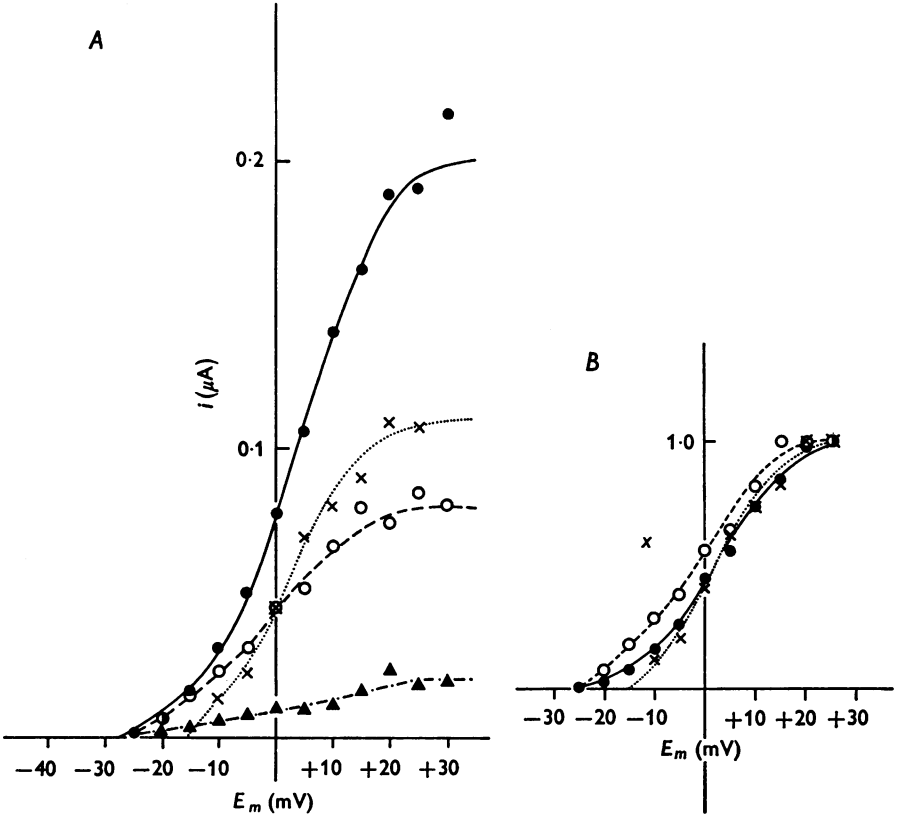

Fig. 7. Activation curves for $i_{x_{fast}}$, $i_{x_{slow}}$ and $i_{x_{total}}$ obtained by the method of three component analysis shown in Fig. 6*A*. *A*, non-normalized activation curves, $x_{total}(E_m)$ (filled circles, continuous line), $x_{slow}(E_m)$ (open circles, interrupted line). $x_{fast}(E_m)$ (crosses; dotted line). Also shown is the amount of positive i_{K_1} accumulation current subtracted at each value of E_m (filled triangles; dot-dash line). *B*, normalized activation curves for the same experiment. Symbols are identical to those shown in Fig. 7*A*. For discussion see text.

Huxley, 1952). Values of $1/\tau$ for the experiment associated with Fig. 7 are shown in Fig. 8. From -20 to $+30$ mV the values of $1/\tau$ were obtained by the 'envelope of tails' method and it will be seen that the curve for $1/\tau_{x_{slow}}(E_m)$ rises slightly more steeply than does the relationship $1/\tau_{x_{total}}(E_m)$. $1/\tau_{x_{fast}}(E_m)$ is not plotted since the sigmoid shape of the tail

'envelope' of $i_{x_{fast}}$ means that kinetic information for this component alone is not easily analysable. Between -30 and -80 mV, $1/\tau_{x_{slow}}$ was measured from the time constant of decay of the directly recorded pacing current using semilogarithmic analysis.

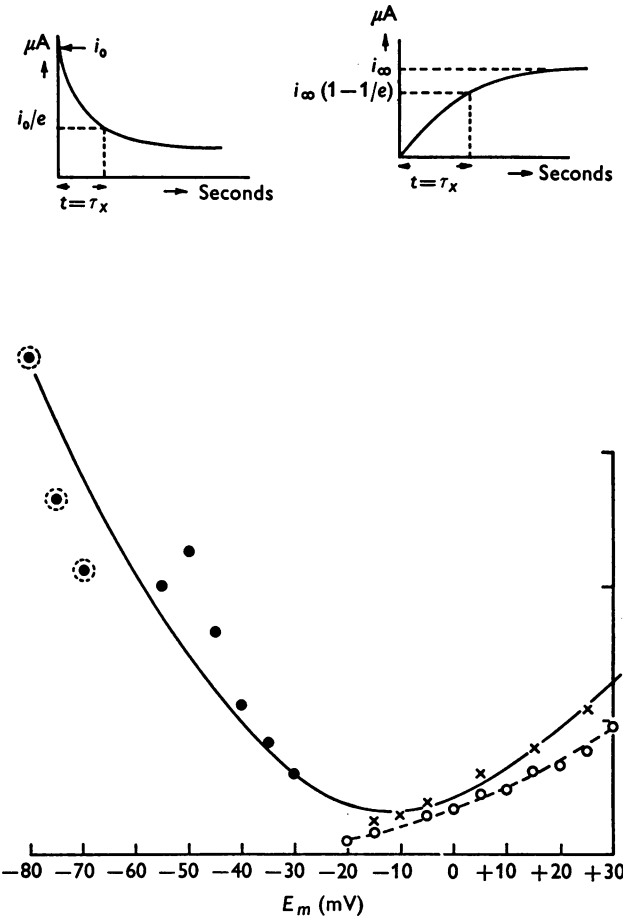

Fig. 8. These results show how kinetic information can be obtained from analysis of positive tails. The experiment involved is the same which gave the results shown in Fig. 7. For membrane potentials between -20 and $+30$ mV (bottom right) estimates of $1/\tau_{x_{total}}(E_m)$ (open circles; interrupted line) and $1/\tau_{x_{slow}}(E_m)$ (crosses; continuous line) have been obtained using 'envelope of tails' analysis (see upper right hand corner). For potentials between -30 and -80 mV (bottom left) estimates of $1/\tau_{x_{slow}}(E_m)$ were obtained from semilogarithmic analysis (upper left hand corner) of the directly clamped pace-maker current (filled circles; continuous line). The circled points are those obtained by estimating the time constant of decay of the pacing current below the reversal potential of $i_{x_{slow}}$ and are therefore likely to be somewhat inaccurate (see text).

It will be seen that the $1/\tau_x(E_m)$ relationship for frog atrial outward currents appears to have the characteristic U-shaped generally associated with the conductance systems of excitable membranes. However, there must be some doubt about the accuracy of a number of points plotted on the left hand side of the U-shaped curve shown in Fig. 8. Below its reversal potential, which in this preparation was about -60 mV, measurement of $\tau_{x_{slow}}$ is more complicated. In order to obtain as full a picture as possible of the kinetic dependence of x we must, therefore, turn to another series of experiments.

2. *Negative tail analysis*

It was shown in the preceding paper (Brown *et al.* 1976*a*, Fig. 3) that when the pacing current, $i_{x_{slow}}$, is clamped below its reversal potential, two phases of negative current decay occur. If Hodgkin–Huxley kinetics are to be obeyed, the time constant of decay of $i_{x_{slow}}$ should decrease quite sharply at negative potentials. The slowly decaying phase of the negative tail is thus unlikely to be identifiable with $i_{x_{slow}}$ since this would give a most uncharacteristic shape to the $1/\tau_{x_{slow}}(E_m)$ relation. However, since we have no *a priori* reason for supposing that the fast phase of current decay represents $i_{x_{slow}}$ alone, we have been cautious about using direct measurements of negative tails to determine the kinetic behaviour of the conductance systems at very negative values of E_m. This caution is further justified by the observation that following square-voltage clamp depolarizations into the 'plateau' potential range, this slow phase of negative current decay is also present in the repolarization tails when the holding potential lies below the zero current level. For these reasons some quantitative and some qualitative information about the behaviour of the i_x currents at negative potentials has had to be obtained from the two indirect methods described below.

A. Qualitative observations. The results from the first type of experiment to be described simply indicate the direction in which $\tau_{x_{slow}}$ changes at negative potentials. The experimental method is illustrated in Fig. 9. An atrial preparation was induced to pace-make and during the repolarization of the action potential, the voltage clamp was switched on for a short time (100–300 ms) hyperpolarizing the membrane to some fairly negative value. The clamp was then switched off again and any change in diastolic interval noted. The voltage clamp pulses shown in Fig. 9 (hyperpolarizing to -70 and -90 mV) both shortened the diastolic interval, the effect of the hyperpolarization increasing with its magnitude. This effect could be explained if the sodium inactivation variable, h, lowered the sodium threshold by being more rapidly reactivated at the negative potentials. The firing threshold of the second and successive action potentials was

definitely shifted to more negative levels by the hyperpolarization (compare control; Fig. 9*A* with Fig. 9*B* and *C*). However an additional factor may also be operating. If the pace-maker current, $i_{x_{slow}}$, decays more rapidly at the negative potentials imposed by the voltage clamp hyperpolarizations, there would be less outward current remaining to decay. This would also enable the membrane to reach the firing threshold sooner. It seems probable that both these effects are operating and that $\tau_{x_{slow}}$ decreases at negative potentials.

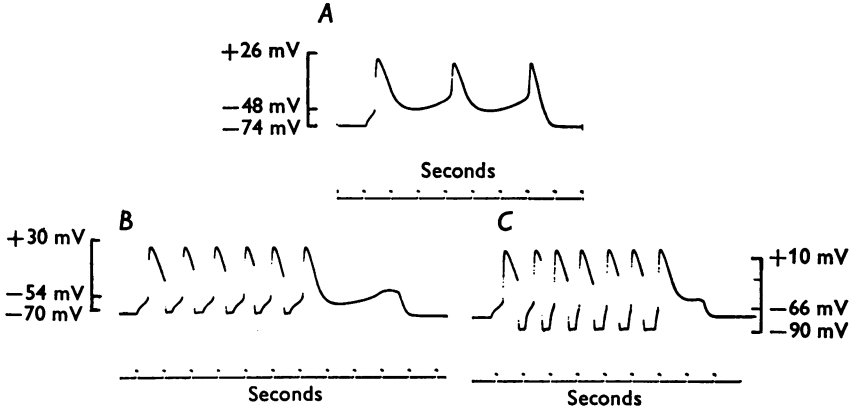

Fig. 9. The effect of voltage clamp hyperpolarization on the rate of induced repetitive activity. *A*, control. The membrane is producing an action potential about once every 2·0 s when depolarized from −74 to −48 mV. *B*, when a hyperpolarizing clamp pulse to −70 mV is applied during the repolarizing phase of the action potential the firing frequency increases to give a diastolic interval of about 730 ms at −54 mV. *C*, a similar situation to that shown in Fig. 9*B* but the hyperpolarization now takes the membrane to −90 mV. Under these conditions the diastolic interval is further reduced to about 550 ms at −66 mV. Note that the maximum diastolic potential increases with the magnitude of the hyperpolarization. These voltage clamp hyperpolarizations have been applied by manual operation of a switch. This explains the irregularity in timing and duration of successive pulses.

This conclusion is supported by observations made under more conventional voltage clamp conditions, where the short hyperpolarization was applied during a positive current decay tail (Fig. 10). A preparation was clamped at a holding potential (−57 mV) at which large positive current tails could be recorded following square depolarizing pulses (E_m = +17) of 1·0 s duration. 250 ms after termination of the depolarization, a negative-going pulse (to E_m = −97 mV) was superimposed on the positive tail for 150 ms. The height of the remaining decay tail after the hyperpolarization was almost zero indicating that holding the membrane

at a negative potential for a short time very substantially increased the rate of decay of outward current. Since the negative pulse was not imposed until the positive current tail had been decaying for 250 ms, the majority of the current affected by the hyperpolarization would probably have been $i_{x_{slow}}$ and $i_{accumulation}$. It therefore seems likely that both these components must decay very much more rapidly at -97 mV than they do at -57 mV.

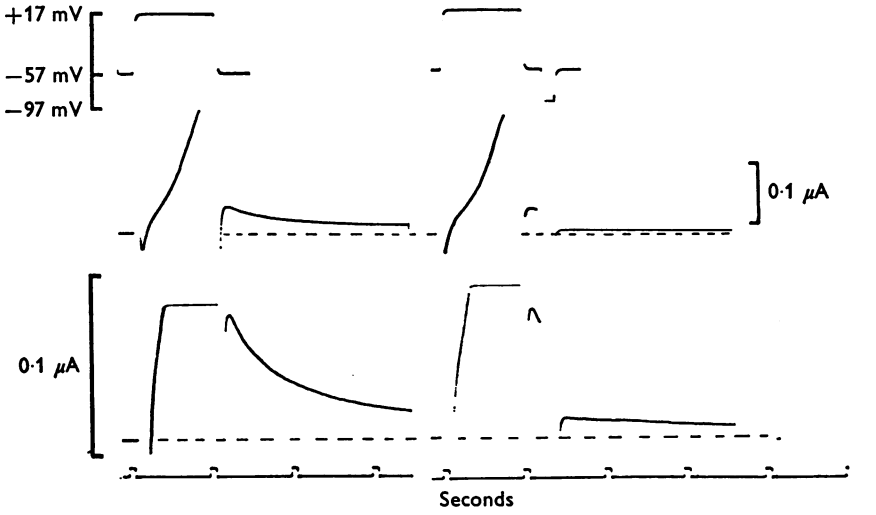

Fig. 10. Experiment to show that τ_x decreases at negative potentials. Upper trace: left hand side: single control pulse. Depolarizing from -57 to $+17$ mV for 1·0 s. Right hand side: double test pulse. Depolarizing from -57 to $+17$ mV for 1·0 s and then, after 250 ms repolarization time, hyperpolarizing to -97 mV for 150 ms. Middle trace: corresponding low gain current records. Note the sigmoid onset of current during the initial depolarization (right-hand current onset slightly retouched). Bottom trace: corresponding high gain current records showing current decay tails only. Following the 150 ms hyperpolarization to -97 mV the current remaining is only 24% of the control value. In both the middle and bottom traces interrupted lines represent the steady-state current level at -57 mV.

B. Quantitative observations. Experiments of the type just described can be extended to provide quantitative data about the behaviour of τ_x at very negative potentials. The method is the same as that shown in Fig. 10 except that both the delay between the onset of the positive tail and the beginning of the hyperpolarization (t_1) and the duration of the hyperpolarizing (t_2) were varied. This point is brought out in Fig. 11 which shows a hypothetical record. The voltage changes are given at the top of the Figure and the associated current changes below. Indicated upon the

current record are the measurements which were made in each case: a is the magnitude of the positive tail immediately preceding the negative pulse and b is the height of the positive tail immediately following hyperpolarization. For each potential to which the negative pulse took the membrane (E_{m_2}) we plotted log b/a ($= \%$ of current decay at E_{m_2}) against t_2 (the duration of the negative pulse). For the simplest case, where only one current component is involved, these points should fall on a straight line where log $b/a = 1$ when $t_2 = 0$ and which decays with a time constant equal to τ_x at E_{m_2}. In order to attempt to eliminate i_{xtast} from the current decay tail, the value of t_1 was varied in several experiments. However, as

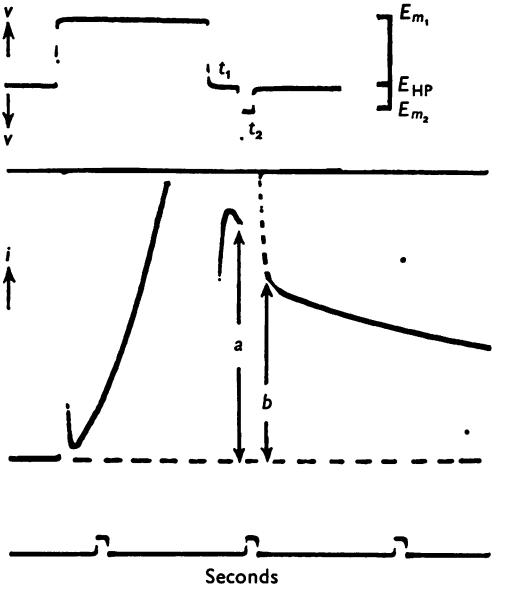

Fig. 11. Diagram of the method used to estimate τ_x at negative values of E_m. All such experiments were done in Ringer + TTX (5×10^{-7} g/ml). Top: voltage protocol. A square-voltage clamp depolarization is given from the holding potential, E_{HP} to E_{m_1}. This depolarization lasts about 1·0 s. The membrane is then repolarized to E_{HP} for time t_1 after which a hyperpolarizing pulse to E_{m_2} is given for time t_2. The membrane is then returned to E_{HP}. Bottom: current protocol. Following depolarization to E_m, a large positive tail is recorded at E_{HP}. After this current has decayed for time t_1 its absolute magnitude, a, is measured. Following hyperpolarization to E_{m_2} for time t_2 the magnitude, b, of the current tail recorded on return to E_{HP} is also measured. The ratio log b/a when plotted against t_2 gives the value of τ_x at E_{m_2}. In some experiments return to the holding potential E_{HP} after hyperpolarization to E_{m_2} gives rise to a spike-like artifact. This is indicated by the vertical interrupted line. Measurement of b is then somewhat more complicated. See text for discussion.

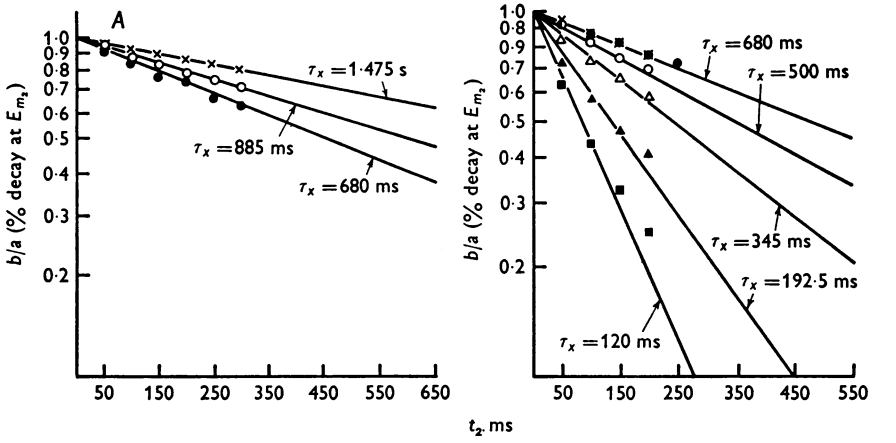

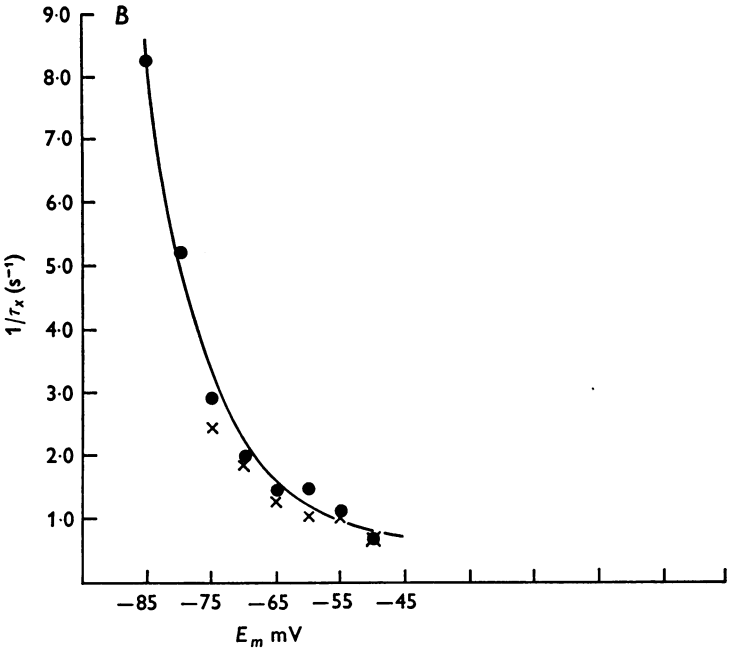

Fig. 12. Results of an experiment designed to estimate τ_x at negative values of E_m. *A*, plots of log b/a against t_2 for different values of E_{m_2}. Right: $E_{HP} = -55$ mV. Values for E_{m_2} are -60 mV (filled circles), -65 mV (crosses), -70 mV (open circles), -75 mV (open triangles), -80 mV (filled triangles), -85 mV (squares). Left: $E_{HP} = -45$ mV. Values for E_{m_2} are -50 mV (crosses), -55 mV (open circles), -60 mV (filled circles). *B*, comparison of the $1/\tau_x$ values obtained in Fig. 12*A* (filled circles) with measurements of $1/\tau_{x_{slow}}$ obtained from the directly clamped pace-maker current (crosses). See text for discussion.

described below, this attempt was not consistently successful. All these experiments were done in the presence of TTX (5×10^{-7} g/ml.) to eliminate sudden increases in sodium conductance associated with depolarization of the membrane to the sodium threshold. Even in the presence of TTX a very rapidly decaying artifact was sometimes present. We do not know the nature of this artifact. It decayed very rapidly but when it was present it was necessary to measure b as the height from the base line to the point at which the rate of decay of the positive tail became slower (i.e. *darker* on the heat sensitive pen recording). The spike like appearance of the artifact is illustrated by the interrupted line in Fig. 11.

Fig. 12 shows the results of such an experiment. The values of τ_x at E_{m_2} measured by plotting log b/a against t_2 (Fig. 12*A*) showed a good correspondence with values of the pacing current decay measured by the direct voltage clamp method over the same potential range (Fig. 12*B*). (It should be noted that both the pacing range and the reversal potential of $i_{x_{\text{slow}}}$ were more negative than is usual in this preparation. The resting potential was also more negative and equal to -87 mV).

All such experiments did not, however, give simple results. In particular we found a number of cases where the line corresponding to τ_x at E_{m_2} would not meet the origin at 1 but converged at a point some way beyond it, at about $t_2 = -100$ ms. This is the kind of result which we might expect for a *two* component system where the rates of deactivation of the components at negative potentials are unequal and become more so as E_{m_2} increases. Thus, if a contained relatively large amounts of $i_{x_{\text{fast}}}$ and $i_{x_{\text{slow}}}$ while b, following short hyperpolarization, contained a relatively greater proportion of $i_{x_{\text{slow}}}$ the ratio log b/a would not vary linearly for small values of t_2. Only when all the $i_{x_{\text{fast}}}$ had decayed at E_{m_2} could the log (b/a) (t_2) relationship theoretically become a straight line. Moreover, the presence of $i_{\text{accumulation}}$ also made itself apparent. Thus, even in those experiments where log b/a could reasonably be extrapolated to 1 when t_2 was zero, it was quite often observed that the individual points recorded after short hyperpolarization tended to fall below the line of best fit, while those corresponding to longer hyperpolarizations fell above it. Therefore, the log (b/a) (t_2) relations were frequently slightly curved. However, the results of these experiments definitely support the view that the rate of decay of the i_x systems ($i_{x_{\text{slow}}}$ together with varying amounts of $i_{x_{\text{fast}}}$ and $i_{\text{accumulation}}$) increases at negative potentials.

3. *Kinetics of i_x systems at positive and negative potentials*

The shape of the $1/\tau_x(E_m)$ relation can now be estimated over a wide range of potentials. In Fig. 13, $1/\tau_{x_{\text{total}}}$ is plotted against E_m using the results obtained in a single preparation but by two different methods. It

will be seen that the points positive to -50 mV for $i_{x_{total}}$ were obtained from the analysis of positive current tail 'envelopes' (those shown in Fig. 4). Points negative to -55 mV were obtained using the method just described. In this particular preparation the pacing current was also clamped directly at potentials between -60 and -40 mV and decayed within this range with a time constant which hardly varied and was about 1·0 s. This fact is taken into account by the position of the

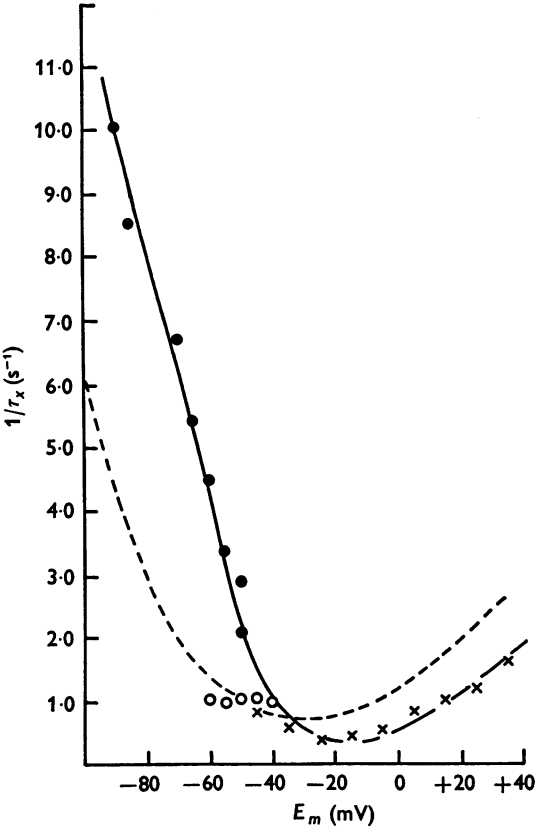

Fig. 13. The shape of the $1/\tau_{x_{total}}(E_m)$ relationship obtained in the same preparation (that giving the results already illustrated in Fig. 4) by two different methods. The crosses indicate the measurements of $1/\tau_x$ obtained from envelopes of positive tails while the filled circles show the values obtained at negative potentials by double pulse analysis of the kind illustrated in Fig. 11. The open circles indicate estimates of $1/\tau_{x_{slow}}$ obtained by directly clamping the pace-maker current between -40 and -60 mV inclusive. These points are taken into account by the interrupted line which is intended to give a very rough estimate of the position of the $1/\tau_{x_{slow}}(E_m)$ curve. The reasons for placing this curve as shown are given in the text.

interrupted line which shows a possible shape for the $1/\tau_{x_{slow}}(E_m)$ relationship. In drawing this curve information about the behaviour of $\tau_{x_{slow}}$ at positive potentials obtained from the experiment associated with Fig. 8 is also taken into account. Again, *direct* information about the behaviour of $\tau_{x_{slow}}$ below its reversal potential (see Noble, S. J., 1976) suggests that at $E_m = -80$ mV, $1/\tau_{x_{slow}}$ is unlikely to be greater than about $3{\cdot}5\ s^{-1}$, slightly higher than the value indicated in Fig. 13.

4. *The fully activated current, $\bar{i}_x$*

It is well known that inward-going rectification is a property of both the time-independent (i_{K_1}) and two of the time-dependent conductance mechanisms (i_{K_2} and i_{x_1}) in the mammalian Purkinje fibre (Noble & Tsien, 1968 and 1969). It has also been shown to exist in association with the time-independent potassium current in atrial muscle (Rougier *et al.* 1968 & 1969; Brown, Noble & Noble, 1976*b*). We have analysed our results to see if evidence exists for the presence of inward-going rectification associated with the time-dependent outward conductances in atrial muscle.

A useful expression for a time-dependent conductance system is,

$$\Delta i_x = \bar{i}_x . \Delta x,$$

where $\bar{i}$ represents the current when all possible membrane channels are open. If we wish to know whether or not the system shows inward-going rectification we must know how $\bar{i}_x$ varies with E_m. Briefly, if

$$\bar{i}_x = \bar{g}(E_m - E_{rev}), \tag{2}$$

where $\bar{g}$ is a constant, the $\bar{i}_x(E_m)$ relationship will be linear and will not show rectifier properties. However, if over a given range of potentials, the value of g is not constant, then the fully activated current–voltage relation $\bar{i}_x(E_m)$ will be non-linear as may occur when inward-going rectification is present.

As was shown in an earlier paper (Brown & Noble, 1969*b*) it is helpful to distinguish between the time-dependent current (i_A) developing during a depolarization from E_{HP} to E_m, and the time-dependent current (i_B) which decays on repolarization to E_{HP}. We may then write

$$\bar{i}_x(E_m) = i_A/\Delta x, \tag{3}$$

where Δx is the fraction of the total current channels which are activated at E_m. We have used this equation to determine values of $\bar{i}_x(E_m)$ in several experiments where the potassium accumulation has been kept as low as possible. The values of i_A used were therefore those associated with depolarizations to E_m which produced the largest recordable positive current tails (see Fig. 4). Because these values of i_A are not necessarily those which correspond to maximal activation of i_x at E_m the method inevitably

causes some error but it is unlikely that this would materially alter the results, an example of which is shown in Fig. 14. These show that inward-going rectification is almost certainly present and that the minimal outward conductance occurs somewhere between about -20 and $+20$ mV. In this preparation the value for minimal conductance was near -15 mV. However, since this corresponds to a situation in which $\bar{i}_x = \bar{i}_{x_{fast}} + \bar{i}_{x_{slow}}$ at $[K]_o > 2$ mM, it is not possible to say either whether its rectifier properties belong to one or to both i_x mechanisms or whether the position on

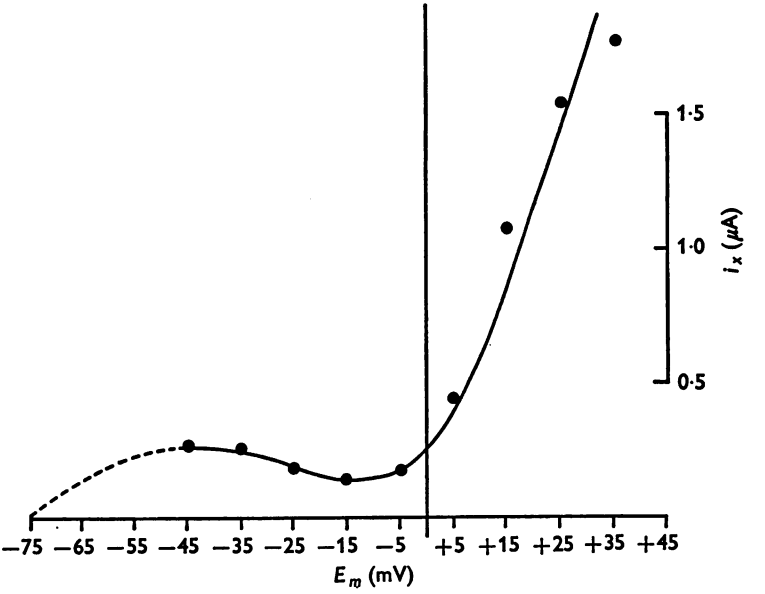

Fig. 14. The fully activated current–voltage relation $\bar{i}_{x_{total}}(E_m)$. The points were obtained by estimating the maximum amount of current activated at a given value of E_m and dividing by the degree of activation, Δx. The inaccuracies involved in using this method are discussed in the text. The interrupted line indicates the shape which the remainder of the curve would have if E_{rev} for $\bar{i}_{x_{total}}$ was close to the zero current level. This is only likely to be the case, however, if a value of $[K]_o$ of approximately 2 mM is assumed.

the voltage axis has been shifted by small, unavoidable increases in $[K]_o$ arising from potassium accumulation. (It will be noticed that part of the curve in Fig. 14 is represented by an interrupted line. Since $\bar{i}_x$ will be zero when i_x is zero, the $i_x(E_m)$ curve must cross the voltage axis at the average reversal potential of $i_{x_{fast}}$ and $i_{x_{slow}}$. This value was estimated at about -75 mV in the absence of accumulation.)

DISCUSSION

In a previous paper we gave evidence for the presence in the membrane of frog atrial wall preparations of three outward current components (Brown *et al.* 1976*a*). These we termed $i_{x_{fast}}$, $i_{x_{slow}}$ and $i_{accumulation}$. As we then showed, $i_{x_{slow}}$ contributes to repolarization of the action potential and its decay underlies the diastolic depolarizations present in trabeculae showing induced pace-maker activity.

In the present paper a quantitative analysis of $i_{x_{slow}}$ is presented. The accuracy of the method of semilogarithmic analysis we have used to separate the three current components ($i_{accumulation}$, $i_{x_{slow}}$ and $i_{x_{fast}}$) from positive current decay tails may be questioned. We have tried to show that inaccuracies due to visual assessment of the i_3 (potassium accumulation) line are minor compared with the large changes in the magnitudes and time constants of $i_{x_{fast}}$ and especially of $i_{x_{slow}}$ which would result from ignoring the accumulation component (see Fig. 6 and related text). Quantitative analysis of $i_{x_{slow}}$ suggests that this component behaves as a time and voltage-dependent Hodgkin–Huxley mechanism. Thus the position of its reversal potential is predictable, always lying about 10 mV positive to the resting potential of the preparation (see Noble, 1976); activation of $i_{x_{slow}}$ rises steeply at potentials positive to between -50 and -30 mV; the activation curve, $x_{slow}(E_m)$, obtained after separation of other outward current components, has the sigmoid shape expected for a conductance mechanism (Fig. 7); and furthermore $i_{x_{slow}}$ appears to have a simple U-shaped $1/\tau(E_m)$ relationship (Figs. 8 and 13).

The very slow outward current component, $i_{accumulation}$, is not thought to be carried by a membrane conductance mechanism but to be caused by the accumulation of potassium ions in extracellular spaces. Its properties are fully discussed elsewhere (Noble, 1976).

The other component of outward membrane current analysed in the present paper is $i_{x_{fast}}$. Although this component is termed $i_{x_{fast}}$ it must be remembered that the subscript 'fast' refers to the rate of decay of this current at negative membrane potentials. By contrast, its onset at positive potentials is apparently much slower than the component we have designated $i_{x_{slow}}$. Thus when the voltage clamp is applied to our preparations during an action potential, no $i_{x_{fast}}$ is recorded, only $i_{x_{slow}}$ alone. $i_{x_{fast}}$ would therefore appear to have no function in normal repolarization and for this reason we originally considered that this current might be a non-uniformity artifact arising when the preparation was strongly depolarized. A rapidly deactivating component might then appear in current decay tails and this component could show all the known characteristics of $i_{x_{fast}}$.

Computer calculations have, however, led us to reject this possibility (Brown *et al.* 1976*b*).

Two questions concerning $i_{x_{fast}}$ thus present themselves. Is $i_{x_{fast}}$ carried by a membrane conductance mechanism and, if so, is its activation really as sigmoid as it seems to be? $i_{x_{fast}}$, like $i_{x_{slow}}$, appears to have a distinct activation range and the total amount of outward current contributed by this component at steady-state activation seems considerable (Fig. 7*A*). However, from our results alone it is impossible to determine conclusively whether the $i_{x_{fast}}$ current represents a genuine conductance mechanism. Thus although the reversal potential of $i_{x_{fast}}$ also appears to lie close to the zero current level (i.e. to E_R), the presence of potassium ion accumulation or depletion and of $i_{x_{slow}}$ deactivation prevents conclusive determinations from being made. The sigmoid onset of $i_{x_{fast}}$ (Figs. 1 and 2) makes determination of its time constants of activation complicated. DeHemptinne (1971) has found that the activation of a time-dependent outward current in *R. esculenta* atrium is sigmoid ($\gamma = 2$ or $\gamma = 3$: see eqn. (1)) and by using appropriate equations has completed its kinetic analysis. Unfortunately, we cannot attempt such a full analysis since we find that $i_{x_{fast}}$ is definitely not activated alone but always with $i_{x_{slow}}$. As will be clear from the Results section, the presence of potassium ion depletion has so far prevented us from obtaining reliable rate coefficients for the latter component and its kinetic properties cannot therefore be fully separated from those of $i_{x_{fast}}$.

In our preparations, a rapidly decaying inward current appears in the decay tails after voltage clamp depolarizations of less than about 1·0 s duration (Fig. 2*A*). This current component is not reduced by manganese ions (3–5 mM) and is therefore unlikely to result from inactivation of the second inward (Ca^{2+}/Na^{+}) current. We have to consider whether the presence of this current, whose nature remains obscure, could cause $i_{x_{fast}}$ activation to appear sigmoid.

Evidence that this is unlikely to be so has been provided recently by the work of Giles (1975). Using a perfusion and recording system identical to our own, Giles has found $i_{x_{fast}}$ to be activated more rapidly in septal preparations taken from the interatrial septum of *R. catesbeiana* than we find in atrial wall trabeculae from the same species of frog. In septal muscle, in contrast to wall muscle, $i_{x_{fast}}$ is recorded as a result of direct voltage clamping of the action potential but its onset, observed here without interference from an initial inward current, is sigmoid.

Giles also records measurable quantities of $i_{x_{fast}}$ at negative holding potentials ($E_{HP} = -60$ mV) following depolarizations into the 'plateau' range of potentials of durations as short as 120 ms. Prolonging the pulse and studying the $i_{x_{fast}}$ 'tail envelope' shows again that the onset of $i_{x_{fast}}$ is sigmoid.

Thus all the available evidence suggests that $i_{x_{fast}}$ is a genuine membrane conductance system in frog atrial muscle. It is activated with a sigmoid time course at potentials within the 'plateau' range in all atrial fibres, but its onset may be more rapid in atrial septal trabeculae than it is in wall preparations. Hence in septal fibres it can be expected to aid repolarization under normal conditions, whereas in wall muscle it probably acts as a safety factor, playing an active role only when the action potential is unduly prolonged.

How do these two components of delayed rectification normally present in frog atrial membrane, $i_{x_{fast}}$ and $i_{x_{slow}}$, compare with those originally described by us in *R. ridibunda* atrium as i_{x_1} and i_{x_2} (Brown & Noble, 1969*a*, *b*) and those Ojeda & Rougier (1974) using *R. esculenta* have termed I_1 and I_2? We think that $i_{x_{fast}}$ and $i_{x_{slow}}$ cannot be directly compared with the i_{x_1} and i_{x_2} of our previous report, for two reasons. Firstly, in our earlier studies, we used a three-electrode recording system which we have subsequently found to cause excessive polarization. Under these conditions misleadingly small amounts of current are recorded, especially when large current changes are involved. Thus, with such a three-electrode system, apparent steady-state current levels were obtained during depolarizations to +25 mV (Brown & Noble, 1969*b*, Fig. 2). By contrast, when using the present four-electrode arrangement (Brown *et al.* 1976*a*, Methods) no steady-state current level can be obtained at potentials positive to about −10 mV. Using three electrodes we also observed a fall in outward current activation during prolonged clamp depolarizations. This fall we attributed to activation below its reversal potential of a second component, i_{x_2} (Brown & Noble, 1969*a*, Fig. 7). Such a fall is apparently also due to electrode polarization since we have never seen similar current 'sags' when using a four-electrode system.

Secondly, the evidence for the presence of i_{x_1} and i_{x_2} was obtained in part from the analysis of *negative* current decay tails. We now find that simple semilogarithmic treatment of such decay tails can be very misleading since the presence of potassium ion depletion interferes with a straightforward Hodgkin–Huxley analysis. The currents we previously described probably do not, therefore, each represent a single system but combinations of at least two components. Thus, under some conditions i_{x_1} represents $i_{x_{fast}}$ together with $i_{x_{slow}}$ and similarly i_{x_2} is probably $i_{x_{slow}}$ combined with $i_{accumulation}$.

The chief differences between Ojeda & Rougier's findings and our own are (1) that they find no sigmoid current onsets, (2) that they are able to obtain steady-state current levels at positive potentials and (3) that they claim that no potassium ion accumulation is present. These differences mean that Ojeda & Rougier have found no obstacle to separating both

current onsets and current decays into one or two exponential processes. Their component I_1 activates rapidly at positive potentials (τ_1 = 0·75 s at −5 mV) and so may, as they point out, play a role in repolarization. At some of the appropriate negative potentials it deactivates too rapidly to control the rate of pace-maker depolarization (τ_1 = approx. 300 ms at −65 mV), though the $1/\tau_{I_1}(E_m)$ relationship is very steep for potentials negative to −35 mV and at −55 mV, where τ_1 = 1·0 s, I_1 decay could support pace-making. The I_1 activation curve, lying between −70 and −20 mV is rather more negative than that which we have found for $i_{x_{slow}}$ in the atrial wall fibres of *R. ridibunda* and *R. catesbeiana* or than those of the outward currents studied by DeHemptinne (1971*a*, *b*) in *R. esculenta* atrium, but corresponds closely with the activation curve obtained by Giles (1975) for $i_{x_{slow}}$ in atrial septal fibres from *R. catesbeiana*. It thus seems likely that $i_{x_{slow}}$ and I_1 are essentially the same component.

Ojeda & Rougier's second outward current, I_2, activates too slowly to contribute to action potential repolarization (τ_2 = approx. 3 s at +25 mV) and deactivates too slowly at negative potentials to underlie pace-maker activity (τ_2 = 3·5 s at −65 mV). Its reversal potential is variable but can be very positive with respect to the resting potential. It seems probable that this component is, at least in part, accounted for by the i_{K_1} current changes resulting from potassium ion accumulation, which are difficult to identify and subtract unless high amplification current records are studied (cf. Brown *et al.* 1976*a*; Noble, 1976).

Although some of these differences in the conclusions drawn by various investigators about atrial outward membrane currents may be due to differences in experimental technique, others may stem from genuine differences between atrial membrane mechanisms in different species of frog and in fibres from different locations within the atrium. Thus apart from the variation in the activation range for the chief repolarization and pace-maker current (I_1 or $i_{x_{slow}}$) there is the evidence of Lenfant, Mirronneau & Aka (1972) that some atrial preparations from *R. esculenta* are extremely resistant to TTX. These trabeculae continue to show induced pace-maker activity in the presence of this drug but not when the second inward current is blocked by manganese ions. This last result complements our own observation that once the second inward current ($i_{Ca/Na}$) is increased by the action of adrenaline, the electrical responses of atrial wall trabeculae from *R. catesbeiana* can appear normal in the presence of TTX (Brown & Noble, 1974).

Are there any general resemblances between frog atrial pace-maker mechanisms and the natural cardiac pace-makers? Two features concerning the behaviour of frog sinus and mammalian sino-atrial node are very

relevant when attempting to answer this question. The first is the observation that the maximal diastolic potential of natural pace-maker regions is relatively low and that the action potentials show little overshoot (Hutter & Trautwein, 1956; Toda, 1968). This implies that any outward pace-maker current must be substantially activated between about -30 and $+5$ mV (I_1 in *R. esculenta* and $i_{x_{slow}}$ in the septum of *R. catesbeiana*) and must decay with a time constant of roughly 1·0–1·5 s between -60 and -40 mV ($i_{x_{slow}}$ in wall trabeculae of *R. ridibunda* and *R. catesbeiana*). The second relevant feature is the strong body of evidence suggesting that cells from the natural pace-maker regions are very TTX insensitive. This evidence is well summarized in Brooks & Lu (1972).

It therefore seems that the characteristics of the pace-maker current whose analysis we have attempted here, are much more likely to mimic those of the natural pace-maker current than are the characteristics of the Purkinje fibre pace-maker conductance, s, previously described by Noble & Tsien (1968). Thus, despite the considerable difficulties involved in analysing the atrial pace-maker current mechanism in a situation in which potassium ion accumulation and depletion also occur, the fact that the 'total' analysis described above reflects the properties of $i_{x_{slow}}$ closely means that this type of preparation can continue to yield useful results, in particular until such time as natural pace-maker tissue can be successfully voltage clamped.

This work was done in Miss R. J. Banister's laboratory and we should like to acknowledge her encouragement and stimulation. Dr A. Clark was supported by a grant from the Mary Goodger fund of Oxford University. Dr S. J. Noble was supported by the Medical Research Council. We should also like to thank the Royal Society for an apparatus grant. We are very grateful to Dr Wayne Giles for helpful discussion.

REFERENCES

BESSEAU, A. (1972). Analyse, selon le modèle de Hodgkin-Huxley, des conductances membranaires du myocarde de grenouille (*Rana esculenta*). *J. Physiol., Paris* **64**, 647–670.

BROOKS, C. McC. & LU, H. H. (1972). *The Sino-atrial Pacemaker of the Heart.* Springfield, Illinois: Charles C. Thomas.

BROWN, H. F., CLARK, A. & NOBLE, S. J. (1976*a*). Identification of the pace-maker current in frog atrium. *J. Physiol.* **258**, 521–545.

BROWN, H. F., NOBLE, D. & NOBLE, S. J. (1976*b*). The influence of non-uniformity on the analysis of potassium currents in heart muscle. *J. Physiol.* **258**, 615–629.

BROWN, H. F. & NOBLE, S. J. (1969*a*). Membrane currents underlying delayed rectification and pace-maker activity in frog atrial muscle. *J. Physiol.* **204**, 717–736.

BROWN, H. F. & NOBLE, S. J. (1969*b*). A quantitative analysis of the slow component of delayed rectification in frog atrium. *J. Physiol.* **204**, 737–747.

BROWN, H. F. & NOBLE, S. J. (1974). Effects of adrenaline on membrane currents underlying pace-maker activity in frog atrial muscle. *J. Physiol.* **238**, 51–52*P*.

DEHEMPTINNE, A. (1971). Properties of the outward currents in frog atrial muscle. *Pflügers Arch. ges. Physiol.* **329**, 321–331.

GILES, W. R. (1975). Electrophysiology of frog atrial muscle. D.Phil. Thesis, Yale University.

HODGKIN, A. L. & HUXLEY, A. F. (1952). A quantitative description of membrane current and its application to conduction and excitation in nerve. *J. Physiol.* **117**, 500–544.

HUTTER, O. F. & TRAUTWEIN, W. (1956). Vagal and sympathetic effects on the pacemaker fibres of the sinus venosus of the heart. *J. gen. Physiol.* **39**, 715–733.

LENFANT, J., MIRRONEAU, J. & AKA, J. K. (1972). Activité répétitive de la fibre sino-auriculaire de grenouille: analyse des courants membranaires responsable de l'automatisme cardiaque. *J. Physiol., Paris* **64**, 5–18.

NOBLE, D. (1972). Conductance mechanisms in excitable cells. In *Biomembranes*, vol. 3, ed. KREUZER, F. & SLEGERS, J. F. G. New York: Plenum Press.

NOBLE, D. & TSIEN, R. W. (1968). The kinetic and rectifier properties of the slow potassium current in cardiac Purkinje fibres. *J. Physiol.* **195**, 185–214.

NOBLE, D. & TSIEN, R. W. (1969). Outward membrane currents activated within the plateau range of potentials in cardiac Purkinje fibres. *J. Physiol.* **200**, 204–231.

NOBLE, S. J. (1976). Potassium accumulation and depletion in frog atrial muscle. *J. Physiol.* **258**, 579–613.

OJEDA, C. & ROUGIER, O. (1974). Kinetic analysis of delayed outward currents in frog atrium. Existence of two kinds of preparation. *J. Physiol.* **239**, 51–73.

ROUGIER, O., VASSORT, G. D., GARGOUIL, Y. M. & CORABOEUF, E. (1969). Existence and role of a slow inward current during the frog atrial action potential. *Pflügers Arch. ges. Physiol.* **308**, 91–110.

ROUGIER, O., VASSORT, G. D. & STÄMPFLI, R. (1968). Voltage clamp experiments on frog atrial heart muscle fibres with a sucrose gap technique. *Pflügers Arch. ges. Physiol.* **301**, 91–108.

TODA, N. (1968). Influence of sodium ions on the membrane potential of the sino-atrial node in response to sympathetic nerve stimulation. *J. Physiol.* **196**, 677–691.